RadioGraphics

Anatomic and Functional Imaging of Metastatic Carcinoid Tumors[1]

Andrew F. Scarsbrook, FRCR • Arul Ganeshan, MRCP • Jane Statham, DCR • Rajesh V. Thakker, FRCP • Andrew Weaver, FRCR • Denis Talbot, FRCP • Philip Boardman, FRCR • Kevin M. Bradley, FRCR Fergus V. Gleeson, FRCR • Rachel R. Phillips, FRCR

ONLINE-ONLY CME

See www.rsna.org/education/rg_cme.html.

LEARNING OBJECTIVES

After reading this article and taking the test, the reader will be able to:

- Identify the clinicopathologic features of carcinoid tumors.
- Recognize the imaging manifestations of carcinoid tumors, especially the expected and atypical patterns of metastasis.
- Describe the role of various imaging modalities in diagnosis, monitoring, and assessment of the treatment response of carcinoid tumors.

TEACHING POINTS

See last page

Carcinoid tumors are a fascinating group of neuroendocrine neoplasms that develop either sporadically or as part of an inheritable syndrome. Many tumors arise in the bronchopulmonary or gastrointestinal tract, but a neuroendocrine tumor can arise in almost any organ. The tumors have varied malignant potential depending on the site of their origin, and the clinical manifestations often are nonspecific. Metastases may be present at the time of diagnosis, which often occurs at a late stage of the disease. Imaging plays a pivotal role in the localization and staging of neuroendocrine tumors and in monitoring the treatment response. Imaging is often challenging, and a combination of anatomic and functional techniques is usually required, depending on the tumor type and location. Techniques include ultrasonography, barium studies, endoscopy, computed tomography, magnetic resonance imaging, somatostatin receptor scintigraphy, iobenguane scintigraphy, and, in select cases, positron emission tomography. Coregistration of structural and functional images is often of incremental value for accurate localization of the primary tumor and any metastatic disease. Radiologists must understand the contribution of each imaging modality in the assessment of different neuroendocrine tumors. In addition, knowledge of the optimal technique for each radiologic and radionuclide imaging examination is essential. Familiarity with the protean imaging appearances of both primary and metastatic disease is essential for accurate staging, treatment monitoring, and surveillance. Finally, an understanding of the wide variety of treatment options for patients with carcinoid tumors is vital for optimal management.

Abbreviations: ACTH = adrenocorticotropic hormone, FDG = fluorine 18 fluorodeoxyglucose, MEN 1 = type 1 multiple endocrine neoplasia

RadioGraphics 2007; 27:455–476 • **Published online** 10.1148/rg.272065058 • **Content Codes:** GI NM OI

[1]From the Departments of Radiology (A.F.S., A.G., P.B., F.V.G., R.R.P.), Nuclear Medicine (A.F.S., J.S., K.M.B., F.V.G.), and Clinical Oncology (A.W.), Churchill Hospital, Oxford Radcliffe Hospitals NHS Trust, Headington, Oxford, England; Academic Endocrine Unit, Nuffield Department of Clinical Medicine, Oxford, England (R.V.T.); and Cancer Research UK, University of Oxford, Oxford, England (D.T.). Recipient of a Certificate of Merit award for an education exhibit at the 2005 RSNA Annual Meeting. Received April 6, 2006; revision requested June 29 and received August 21; accepted August 22. All authors have no financial relationships to disclose. **Address correspondence to** A.F.S., Department of Clinical Radiology, St James's University Hospital, Leeds Teaching Hospitals NHS Trust, Beckett St, Leeds, LS9 7TF, England (e-mail: *andrew.scarsbrook@leedsth.nhs.uk*).

Introduction

Teaching Point

Neuroendocrine tumors may arise in a wide range of organs, but they most commonly arise in the submucosa of the bronchopulmonary and gastrointestinal tracts (1,2). Carcinoid tumors are a subgroup of midgut neuroendocrine tumors that secrete serotonin (5-hydroxytryptamine). Although the terms *neuroendocrine tumor* and *carcinoid tumor* are often used interchangeably, in this review we generally have used the term *carcinoid tumor* to describe that specific entity. Approximately 20% of patients with carcinoid tumors have metastatic disease at presentation, and in half of those patients the primary tumor is not located at initial imaging (3).

In the past few decades, the overall incidence of carcinoid tumors has increased, partly because of improved detection rates (1). There are an increasing number of new treatment modalities that may result in a better quality of life and longer survival. Diagnostic imaging plays a pivotal role in the initial assessment of carcinoid tumors and in monitoring their response to therapy. Multidisciplinary collaboration is critical to ensure optimal management in each case.

The article reviews the diverse clinicopathologic and radiologic features of carcinoid tumors. In addition, the imaging features of late-stage complications such as carcinoid heart disease, and the predictable and atypical patterns of metastasis, are highlighted. Anatomic and functional imaging techniques that are used to assess carcinoid tumors are described. Contemporary treatment of metastatic carcinoid tumors is briefly discussed, and the radiologic assessment of response to various treatments is described. Finally, optimal imaging protocols for initial assessment, disease monitoring, and detection of new manifestations of carcinoid tumors are suggested.

Clinicopathologic Features of Carcinoid Tumors

Carcinoid tumors derive from enterochromaffin cells, or Kulchitsky cells, which are widely distributed in the human body (1). These tumors are relatively uncommon, with an annual incidence of 1.2–2.1 per 100,000 persons in the general population (1). Carcinoid tumors traditionally have been classified, according to their derivation from the three embryonic divisions of the gut, as foregut, midgut, and hindgut tumors (4) (Table). There is currently a shift away from this system to a histology-based classification system in which the tumor subtype is determined according to cellular differentiation (5). Because this new system is not yet firmly established, the traditional classification system was used in this article.

Foregut lesions account for 20%–25% of all carcinoid tumors, with most primary lesions being found in the lung, thymus, stomach, or proximal duodenum, and few in the hepatobiliary tract or pancreas (4). Foregut neuroendocrine tumors usually have a low serotonin content but may secrete precursors of serotonin, as well as histamine and polypeptide hormones such as corticotropin-releasing hormone, adrenocorticotropic hormone (ACTH), gastrin, and chromogranin A (6).

Table 1
Site and Frequency of Primary Carcinoid Tumors

Site of Origin	Frequency*
Foregut	
Thymus	1–2
Bronchopulmonary tract	10–25
Esophagus	<1
Stomach	2–30
Duodenum	2–5
Pancreas	<1
Hepatobiliary tract	<1
Midgut	
Jejunum	1–2
Ileum	15–20
Appendix	19–35
Ascending colon	1–5
Hindgut	
Transverse colon	1–5
Descending colon	2–5
Rectum	10–12
Ovary or testis	<1
Unknown	10

*The estimated frequency is given as a percentage of all carcinoid tumors.

Midgut carcinoid tumors, which are considered the classic form of the disease, account for about 40%–50% of cases. They may arise from the distal duodenum, jejunum, ileum, appendix, or proximal colon, with a location in the appendix being the most common. They contain peptides and amines and secrete serotonin (5-hydroxytryptamine), the serotonin precursor 5-hydroxytryptophan, bradykinins, tachykinins, histamine, substance P, ACTH, and chromogranin A (6).

Hindgut tumors account for about 15% of cases and originate in the distal part of the colon and rectum (4). Hindgut neuroendocrine tumors contain hormones such as pancreatic polypeptide, somatostatin, and chromogranin A (6).

Extremely rarely, carcinoid tumors may originate from the kidney (7), middle ear (8), or testis (9). The primary site is unknown in approximately 10% of cases (1,3). Most carcinoid tumors are sporadic; however, syndromal carcinoid tumors (of foregut origin) are associated with type 1 multiple endocrine neoplasia (MEN 1) in about 10% of cases (10) and also occur rarely in type 2 multiple endocrine neoplasia and type 1 neurofibromatosis (11). Urinary 5-hydroxyindolacetic acid, a breakdown product of serotonin, is an important marker of carcinoid disease. Chromogranin A is another sensitive biochemical marker of neuroendocrine tumors, with the plasma level being proportional to the tumor load (12).

Teaching Point

Carcinoid tumors are relatively slow growing, and, even in the presence of metastatic disease, patients can survive for several years with current treatment strategies (3). The overall 5-year survival rate (regardless of tumor site or stage) approaches 70%–80% (13). Appendiceal and bronchial carcinoid tumors are associated with the highest survival rates because of the reduced incidence of invasive growth and metastases in these tumors (3). Conversely, the lowest survival rates (20%–30% at 5 years) are found among patients with poorly differentiated tumors with distant metastatic disease at diagnosis (3).

Overall, 40%–60% of patients are asymptomatic at presentation (14). Foregut and hindgut tumors contain low levels of serotonin and rarely cause symptoms due to vasoactive peptide release (14). Midgut tumors are more commonly symptomatic because of paracrine secretion of peptides into the intestine and resultant diarrhea. Systemic vasoactive peptide release by metastatic tumors (usually of midgut origin) often is manifested by the characteristic symptoms of the carcinoid syndrome: diarrhea; episodic facial and upper body flushing; abdominal cramping; right heart failure; and, less frequently, wheezing (12).

Approximately 50% of patients with the carcinoid syndrome develop carcinoid heart disease, which typically involves the right side of the heart. Abnormalities in cardiac function are caused by the formation of endocardial plaques with fibrous tissue in the tricuspid valve, pulmonary valve, cardiac chambers, venae cavae, pulmonary artery, and coronary sinus (15). The fibrous tissue in the plaques results in distortion of the valves, a condition that leads to valvular stenosis, regurgitation, or both. Between 5% and 10% of patients also develop left-sided valvular disease (16).

Metastatic disease occurs in approximately 30%–50% of patients with carcinoid tumors. Metastases may occur at any time, from long before the diagnosis to 20 years after the initial presentation; 12%–22% of patients have disseminated disease at diagnosis (1). The most common sites of metastasis from midgut carcinoid tumors are mesenteric lymph nodes and the liver. Metastases to the lung, peritoneum, bone, and pancreas are less common. Rare sites of metastasis include soft tissues (17), the breast (18), and the orbit (19).

Radiologic Features of Carcinoid Tumors

Foregut Tumors

Thymic Tumors.—Thymic carcinoid tumors are rare malignant tumors that occur more frequently in male patients (male-to-female ratio, 3:1) (20). They typically are manifested in middle age and are more aggressive than bronchial carcinoid tumors. Thymic tumors may be asymptomatic until they reach a large size. An estimated 50% of thymic tumors may be functionally active, and such tumors most commonly are present with Cushing syndrome (21). In as many as 25% of sporadic cases, a thymic carcinoid tumor may be associated with underlying MEN 1 (20).

Figure 1. Thymic carcinoid tumor. **(a)** CT pulmonary angiogram shows a large, partially enhancing anterior mediastinal mass (arrow) that subsequently was diagnosed as a thymic carcinoid tumor on the basis of biopsy results. **(b)** Axial contrast-enhanced CT image, obtained in a patient with a preexisting diagnosis of thymic carcinoid tumor, depicts metastatic mediastinal, pericardiac, and pleural deposits (arrows).

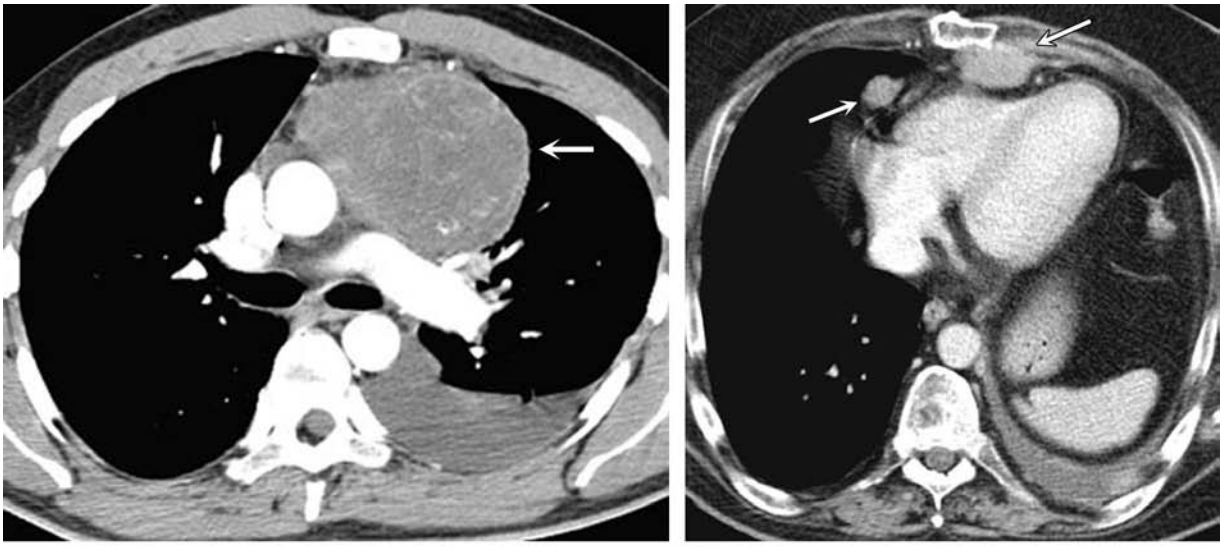

a. **b.**

Cross-sectional imaging of patients with a thymic carcinoid tumor typically depicts a large, well-circumscribed, anterior mediastinal mass that may be indistinguishable from a thymoma (Fig 1a). Thymic carcinoid tumors often are locally invasive and frequently metastasize to regional lymph nodes, the adrenal glands, and bone. Pulmonary, pleural, cerebral, and renal metastases occur less commonly (22). Up to 30% of patients with a thymic carcinoid tumor have advanced-stage disease at presentation (20) (Fig 1b).

Bronchopulmonary Tumors.—Bronchopulmonary carcinoid tumors are classified according to histologic criteria as typical or atypical (23). About 80%–90% of cases are typical bronchopulmonary carcinoid tumors, which generally are low grade and have a benign course (24). The remainder (10%–20%) are atypical tumors, which are much more aggressive and may have metastasized to the liver, bone, adrenal glands, or brain at the time of diagnosis. Atypical bronchopulmonary carcinoid tumors also are associated with a higher rate of recurrence after surgical excision (23). The typical cross-sectional appearance of a bronchopulmonary carcinoid tumor is a spherical or ovoid lesion with well-defined borders and a location close to the central bronchi (25). Small tumors may be entirely intrabronchial (Fig 2a). Up to 30% of bronchopulmonary tumors may contain areas of calcification in a punctate or diffuse pattern (20,24) (Fig 2b). Pulmonary carcinoid tumors occur in the peripheral lung tissue, without evidence of a bronchial relationship, in about 16%–40% of cases (20) (Fig 2c). There is overlap in the imaging appearances of typical and atypical carcinoid tumors, but atypical bronchopulmonary carcinoid tumors are generally larger, may contain a central region of necrosis or hemorrhage, are more commonly located in the periphery of the bronchopulmonary tree, and may be locally invasive (24). ACTH-dependent Cushing syndrome results from ectopic hormone secretion in approximately 2% of patients with a bronchopulmonary carcinoid tumor (23). The responsible tumor is often smaller than 1 cm, and octreotide scintigraphy is very useful for detecting occult tumors in such cases (20,24) (Fig 2d, 2e).

Figure 2. Bronchial carcinoid tumor in four patients. **(a)** CT pulmonary angiogram obtained for evaluation of suspected pulmonary embolic disease shows a small intrabronchial carcinoid tumor in the right main bronchus (arrow) and a thrombus in the left inferior pulmonary artery (arrowhead). **(b)** Contrast-enhanced chest CT image obtained in another patient shows a partial collapse of the lower lobe of the right lung, caused by a calcified atypical carcinoid tumor (arrow). **(c)** Axial thoracic CT image demonstrates a typical bronchial carcinoid tumor in the periphery of the right lung. **(d)** Planar scintigram obtained with indium 111 (^{111}In)-octreotide shows a focal area of radiotracer uptake (arrow) in the right hemithorax. **(e)** CT image obtained in the same patient as **d** shows a small right pulmonary nodule (arrow) that corresponds to the focal area of uptake in **d**. The patient had ectopic ACTH-induced Cushing syndrome due to a functional bronchial carcinoid tumor, which resolved after resection of the nodule. (Figs 2d and 2e courtesy of John Rees, MD, University Hospital of Wales, Cardiff, Wales.)

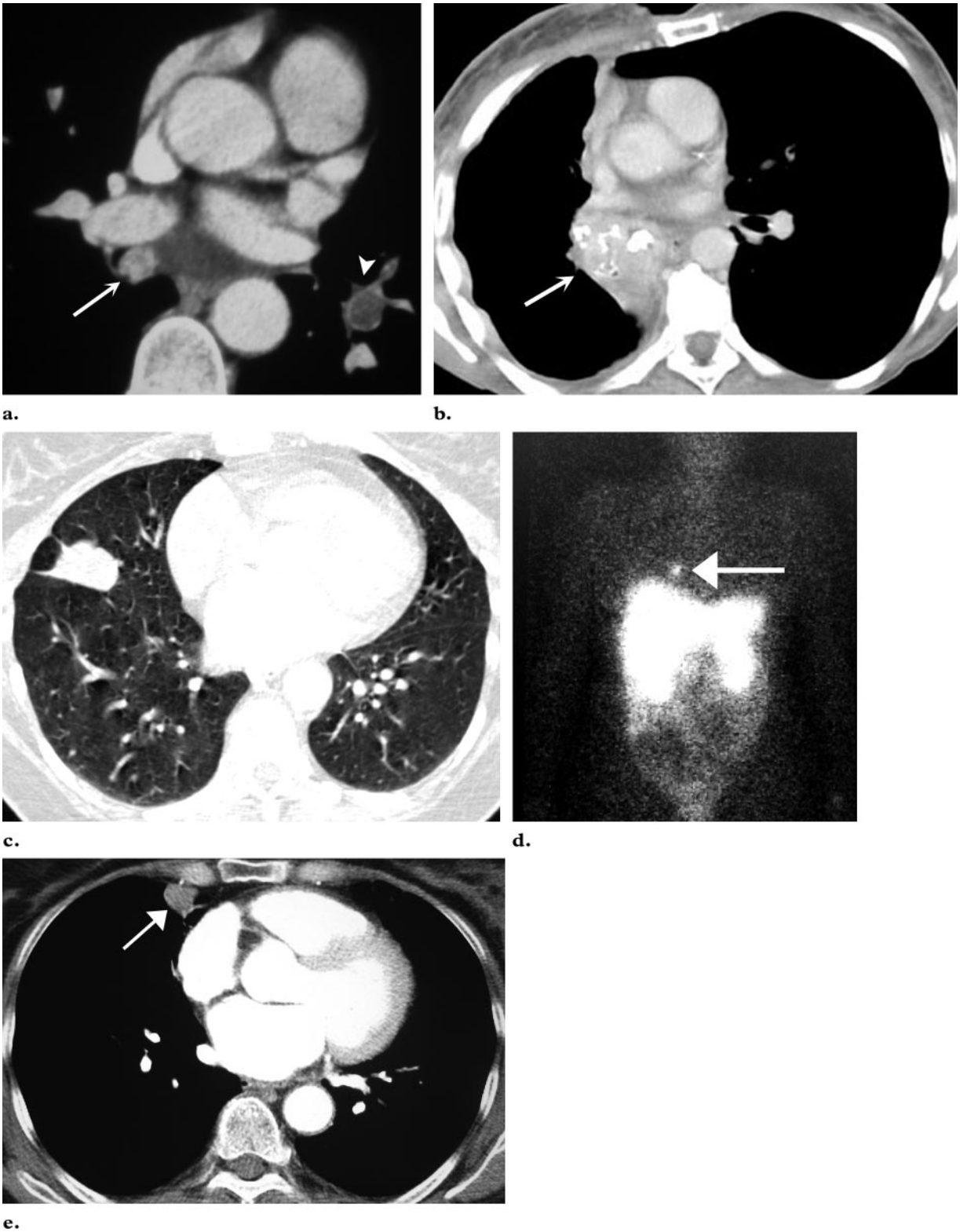

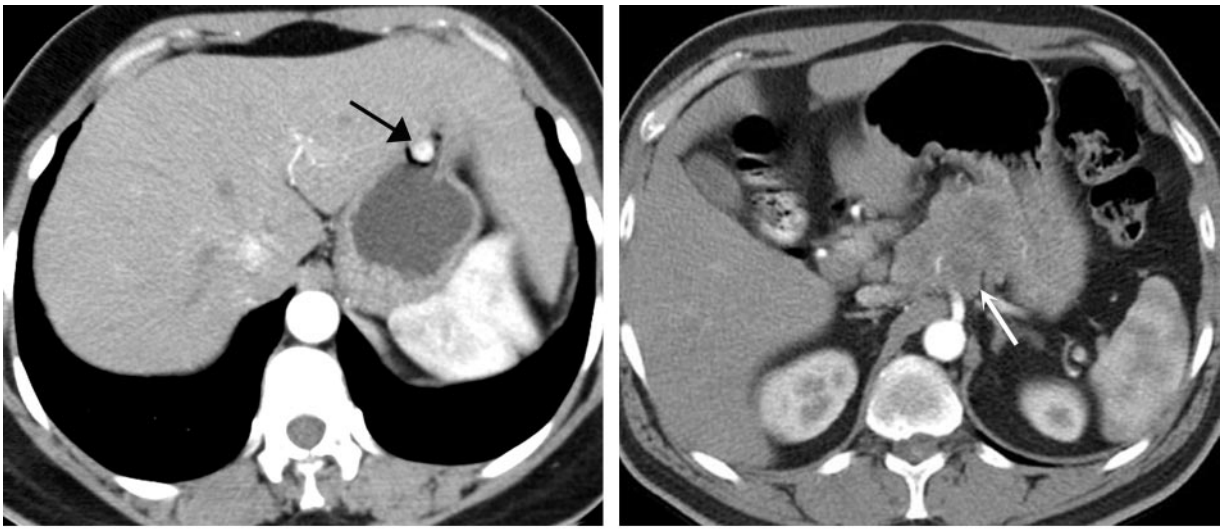

a. b.

Figure 3. Gastric carcinoid tumors. **(a)** Contrast-enhanced arterial phase CT image shows a small avidly enhancing gastric nodule at the lesser curvature of the stomach (arrow). The nodule was histologically proved to be a type I tumor. **(b)** Contrast-enhanced CT image in another patient shows a large heterogeneous locally invasive mass that originated from the gastric cardia and surrounds the adjacent celiac artery (arrow). The tumor was resected and was proved at histologic analysis to be a type III gastric carcinoid tumor.

Positron emission tomography (PET) performed with fluorine 18 fluorodeoxyglucose (FDG) often produces false-negative results due to low metabolic activity within typical carcinoid tumors; however, atypical tumors may demonstrate increased FDG uptake (24,26).

Gastric Tumors.—There are three subtypes of gastric carcinoid tumors, each with different pathologic and prognostic features (27). These tumors also are referred to as gastric enterochromaffin-like (ECL) cell carcinoids (ECLomas). Gastroscopy with multiple biopsies of tumoral and nontumoral tissues is essential for histopathologic distinction between the subtypes.

Type I gastric carcinoid tumor (ECLoma type I) is the most common subtype (70%–80%) and is associated with achlorhydric atrophic gastritis that affects the gastric body (28). Type I tumors are often detected coincidentally at endoscopy performed because of dyspepsia. The lesions consist of multiple small (<1 cm) nodules within the gastric fundus and body (28). Small enhancing mucosal nodules are seen at contrast material–enhanced computed tomography (CT) (27) (Fig 3a). Type I gastric carcinoid tumors are considered benign, and the usual treatment is endoscopic resection (28).

Type II gastric carcinoid tumors (ECLoma type II) are uncommon (5%–10% of cases); they occur almost exclusively in MEN 1 patients with a gastrinoma and hypergastrinemia-associated Zollinger-Ellison syndrome (27,28). The tumors are multicentric and usually are small, but metastases to regional lymph nodes and the liver occur in 10%–30% of cases (28). The appearances of primary lesions on cross-sectional images and images from double contrast barium studies frequently is striking, with multiple masses and associated gastric wall thickening (27). Endoscopic surveillance for tumor development is advisable in patients with MEN 1, and cross-sectional or functional imaging may be necessary to detect nodal or hepatic metastases (27). Treatment options include medical therapy with oral octreotide, which may induce gastric tumor regression in some cases (28).

Type III gastric carcinoid tumors (ECLoma type III) are relatively common (15%–25% of cases), are sporadic, occur in the absence of a pre-

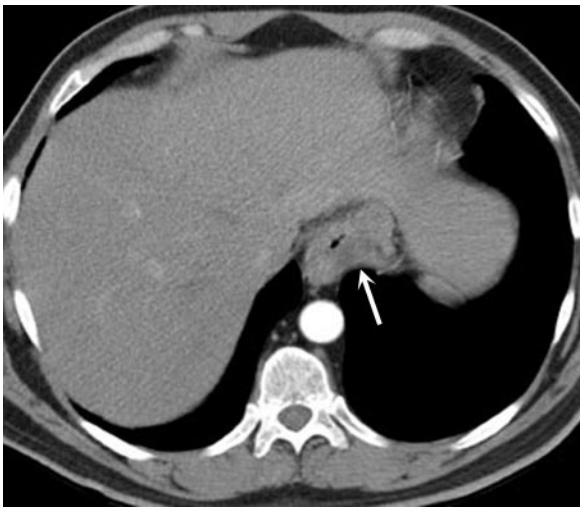

Figure 4. Esophageal carcinoid tumor. Contrast-enhanced CT image shows asymmetric circumferential thickening of the wall of the distal esophagus (arrow), an extremely rare site of carcinoid disease. At endoscopic biopsy, the lesion was found to be a carcinoid tumor.

disposing gastric pathologic condition, and are more common in men (28). Type III tumors generally are solitary, are larger than 2 cm in diameter, and behave more aggressively than do other subtypes (27) (Fig 3b). The occurrence of metastatic disease is dependent on tumor size; however, in many patients, metastases have developed at the time of diagnosis and, consequently, the prognosis is poor, with a 5-year survival rate of approximately 20% (27,28). Cross-sectional imaging and octreotide scintigraphy are important for staging of type III tumors. Treatment of these tumors is more aggressive and is similar to that for gastric adenocarcinoma (28).

Esophageal Tumors.—Esophageal carcinoid tumors are extremely rare, and patients usually present with symptoms of dysphagia. The cross-sectional imaging features of esophageal carcinoid tumors mimic those of esophageal carcinomas (Fig 4).

Duodenal Tumors.—Carcinoid tumors of the duodenum are rare; they account for less than 3% of gastrointestinal neuroendocrine tumors (13). Most duodenal carcinoid tumors are sporadic, nonfunctioning, and arise in the proximal duodenum. However, tumors occasionally may be functioning and may be manifested with Zollinger-Ellison syndrome (29). A small number of patients with duodenal carcinoid tumors have underlying type 1 neurofibromatosis or MEN 1; in particular, approximately 30% of patients with periampullary carcinoid tumors also have type 1 neurofibromatosis (29). Most tumors are discovered coincidentally during endoscopy. Tumors are rarely more than 2 cm in size; however, those that do reach a larger size may metastasize to regional lymph nodes or the liver in 40% of patients (29). Endoscopic ultrasonography (US) is the most sensitive imaging technique for the detection of a duodenal carcinoid tumor. Endoscopic US images typically depict the tumor as a small, polypoid, submucosal lesion (Fig 5), but local tumor invasion and regional nodal involvement also may be seen (30). CT features include focal mural or intraluminal duodenal masses, which may demonstrate early arterial phase enhancement after the intravenous administration of iodinated contrast media (29). Contrast-enhanced abdominal CT or abdominal magnetic resonance (MR) imaging and radiolabeled octreotide scintigraphy are important for accurate tumor staging.

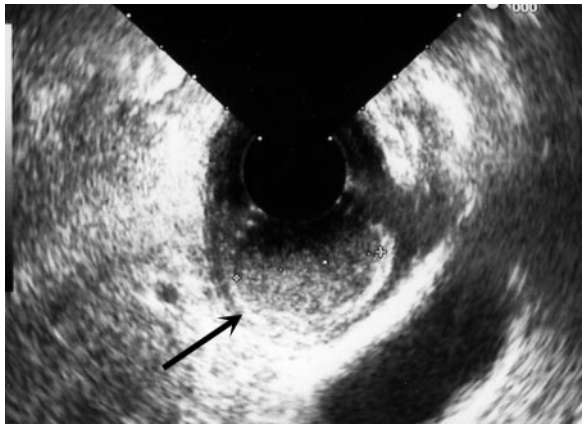

Figure 5. Duodenal carcinoid tumor. Endoscopic US image depicts a 16-mm submucosal polyp in the proximal part of the duodenum (arrow). The polyp was resected endoscopically and diagnosed histologically as a carcinoid tumor. (Courtesy of Jane Phillips-Hughes, MD, Oxford Radcliffe Hospitals NHS Trust.)

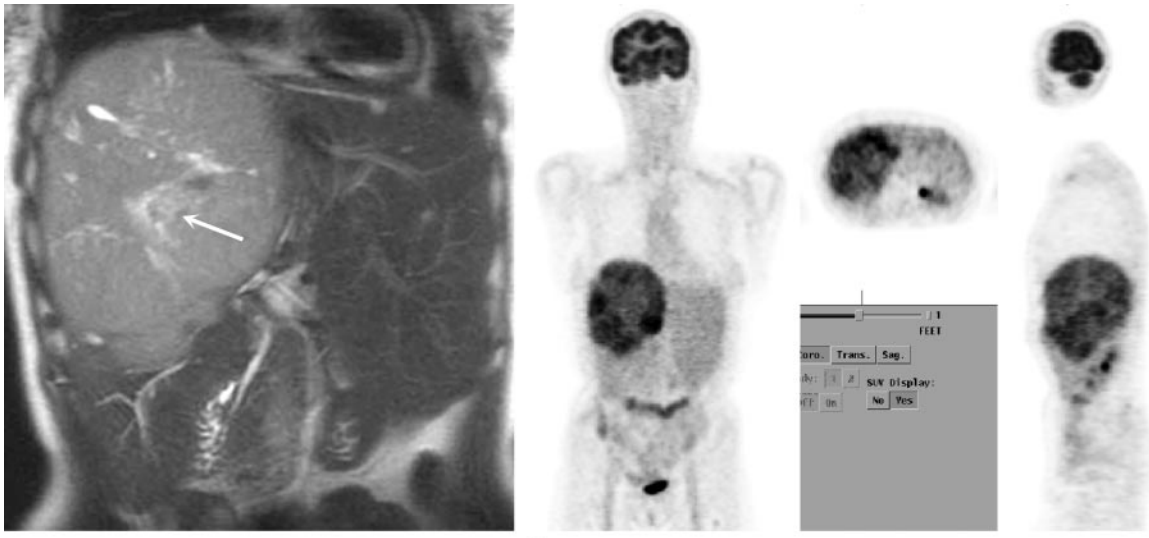

a. b.

Figure 6. Primary hepatic carcinoid tumor. **(a)** Coronal T2-weighted MR image shows a large solid mass in the right lobe of the liver. The mass contains a small area of high signal intensity (arrow) that is indicative of necrosis. At histologic analysis of a biopsy specimen, the mass was proved to be a poorly differentiated carcinoid tumor. After careful evaluation, it was determined that the liver was the primary site of disease. **(b)** Coronal, axial, and sagittal images from FDG PET in the same patient show the large solitary hepatic mass. **(c)** Axial gadolinium-enhanced T1-weighted MR image from another patient demonstrates a tumor with peripheral and septal enhancement.

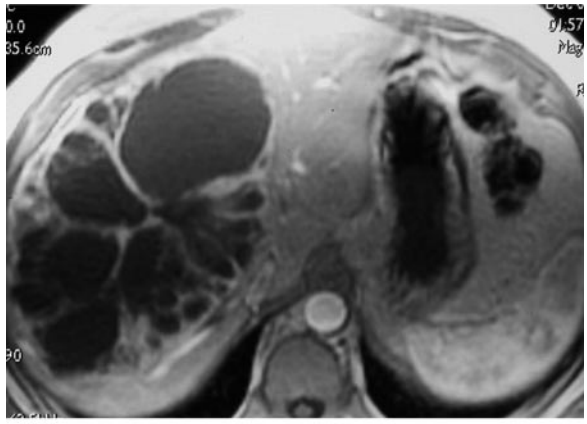

c.

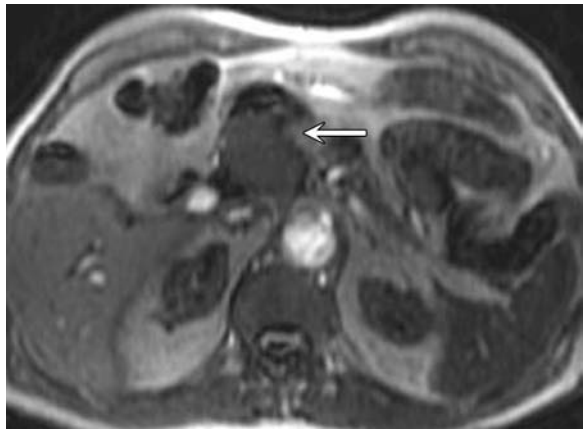

Figure 7. Pancreatic carcinoid tumor. Gadolinium-enhanced T1-weighted MR image shows an intermediate-signal-intensity mass in the head of the pancreas (arrow), a finding that is indistinguishable from pancreatic adenocarcinoma. The results of histologic analysis allowed a diagnosis of pancreatic carcinoid tumor.

Primary Liver Tumors.—Primary hepatic carcinoid tumors are extremely rare. When a carcinoid tumor is found in the liver, great care must be taken to exclude metastasis from an extrahepatic primary site, as that is a much more common occurrence (31). Hepatic carcinoid tumors are slightly more common in women than in men and typically are manifested in middle age. Common symptoms include abdominal pain, and there may be a palpable epigastric mass (31). The cross-sectional imaging features usually consist of a solitary hepatic mass (with or without several small satellite nodules) with a diameter of up to 25 cm (31). A carcinoid tumor in the liver may be solid (60% of cases) (Fig 6a, 6b), partially solid with cystic areas (25% of cases), or mainly cystic (15%, Fig 6c), and may demonstrate peripheral enhancement after the administration of an iodinated contrast agent. Hepatic carcinoid tumors have low signal intensity on T1-weighted images (Fig 6c) and high signal intensity on T2-weighted

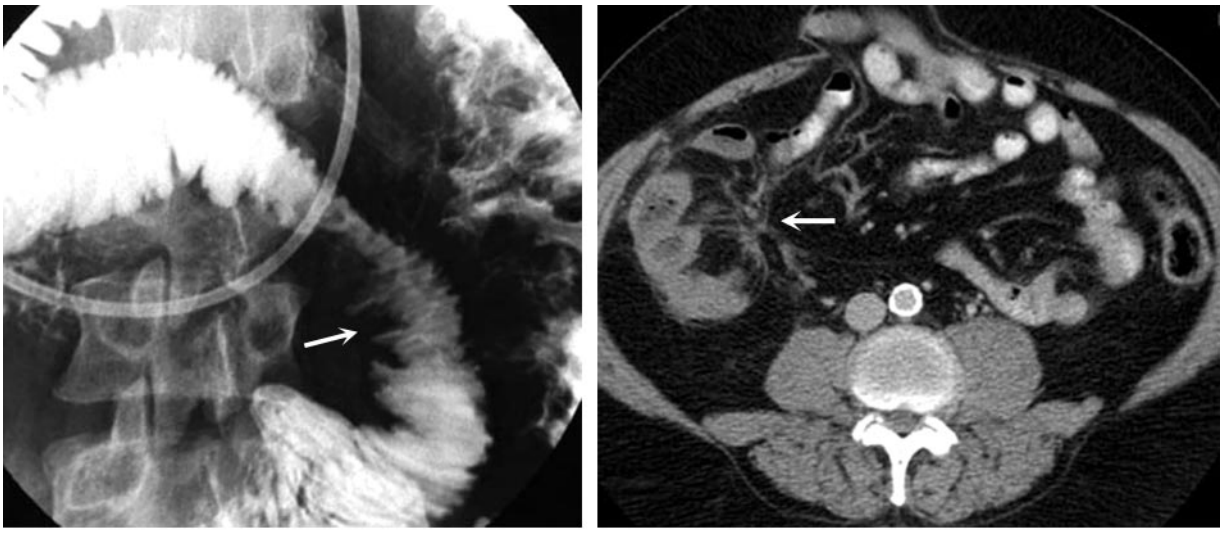

a. b.

c.

Figure 8. Small-bowel carcinoid tumor. **(a)** Image from an enteroclysis study performed in a patient with a midgut carcinoid tumor demonstrates mucosal thickening (arrow), angulation, and fixation of a segment of the distal part of the ileum because of the tumor and associated mesenteric fibrosis. **(b)** Axial CT image in another patient with a distal ileal carcinoid tumor shows an area of desmoplastic reaction in the small-bowel mesentery (arrow). **(c)** Coronal T2-weighted MR image shows a large mesenteric mass with characteristic surrounding mesenteric fibrosis and with thickening of the ileal wall because of ischemia (arrows).

images, and their enhancement characteristics at MR imaging after the administration of an intravenous gadolinium-based contrast agent are similar to those at contrast-enhanced CT.

Pancreatic Tumors.—Primary pancreatic carcinoid tumors are very rare and usually are associated with a poor prognosis, but occasionally they may behave less aggressively (32). Most cases are associated with metastases at diagnosis, and many patients present with the carcinoid syndrome (32). Cross-sectional imaging typically demonstrates a relatively large pancreatic mass that is indistinguishable from other pancreatic tumors (Fig 7).

Midgut Carcinoid Tumors

Small-Bowel Tumors.—Most small-bowel tumors occur in the distal ileum. Multiple primary tumor sites are found in 29%–41% of cases, and a second, unrelated primary malignancy (usually a gastrointestinal or genitourinary tract adenocarcinoma) is found in a significant percentage of patients (6,10). Patients may be asymptomatic or have vague abdominal symptoms for many years and may present at a late stage, after carcinoid syndrome has developed (33). Alternatively, patients may present with a palpable mass, abdominal pain, diarrhea, bowel obstruction, or gastrointestinal bleeding (14). Tumors larger than 2 cm are more likely to be symptomatic and to metastasize (10). Most midgut carcinoid tumors are small and consequently difficult to detect at cross-sectional imaging (34). Small-bowel enteroclysis may demonstrate a submucosal nodule, but primary tumors frequently are not detected (33). More commonly, small-bowel studies may demonstrate thickening, angulation, tethering, and fixation of ileal loops as a consequence of mesenteric fibrosis (Fig 8a). Because of recent advances in multidetector CT technology, small primary tumors sometimes may be depicted, especially if water is used as an oral contrast agent and multiplanar reformatting of image data is performed

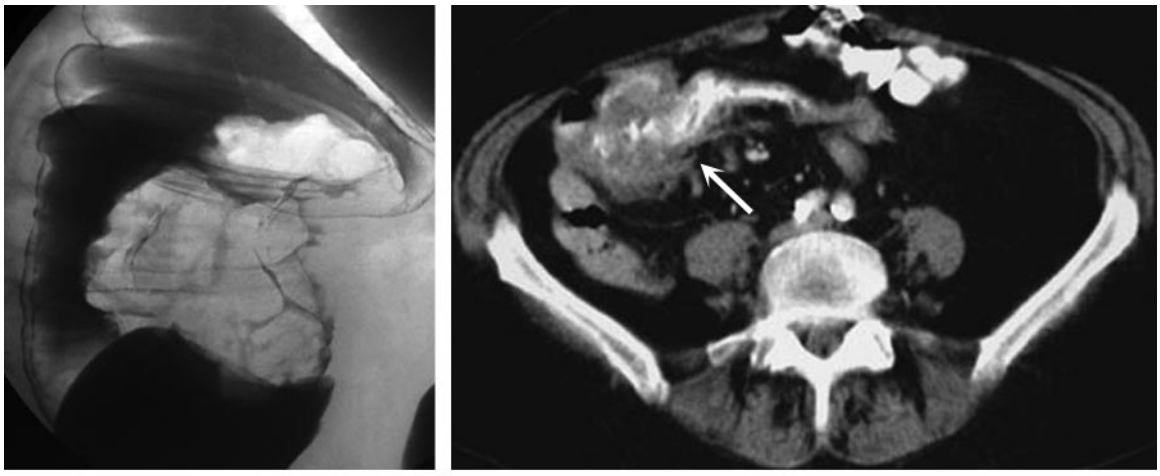

a. b.

Figure 9. Cecal carcinoid tumor. **(a)** Image from a double contrast barium study demonstrates a polypoid cecal mass that was biopsied colonoscopically and proved to be a carcinoid tumor. **(b)** Axial CT image shows circumferential thickening of the cecum (arrow).

(33). At CT, the usual appearance of mesenteric disease is an ill-defined enhancing soft-tissue mass. In an estimated 70% of cases, the mass contains calcification (35). Frequently, even without any direct invasion by the primary tumor, there is a mesenteric desmoplastic reaction due to mesenteric ischemia and fibrosis caused by release of serotonin and other hormones from the tumor (35) (Fig 8b, 8c). Because of this process, the mesenteric vessels may be compromised, with resultant thickening of adjacent bowel loops due to ischemia (36) (Fig 8c). On MR images, carcinoid tumors may be manifested as foci of asymmetric wall thickening with signal isointensity on T1-weighted images and iso- or mild hyperintensity on T2-weighted images (34). Rarely, a well-defined nodular mass may be demonstrated, but, typically, small-bowel carcinoid tumors more often are extremely difficult to detect (37). In contrast, mesenteric involvement and liver metastases, which are common even with small primary tumors, are easily detected at cross-sectional imaging.

Appendiceal Tumors.—Carcinoid tumor is the most common type of appendiceal tumor and is almost invariably discovered incidentally at pathologic examination after appendectomy (in 0.3% of patients who undergo that procedure) (38). Tumors are typically small (in 95% of cases, <2 cm in diameter) and located in the distal third of the appendix (6). Because they are small, most tumors are not detected radiologically. However, larger tumors may be demonstrated and, if calcified, may mimic appendicoliths. The tumors also may be manifested as diffuse mural thickening or as a mesenteric soft-tissue mass due to metastatic disease (39). Tumor size is the best predictor of prognosis: Tumors with a diameter of less than 2 cm almost never metastasize and should be considered benign; treatment with appendectomy is considered curative (38). In contrast, 30% of patients with larger tumors develop nodal or distant metastases, and in these cases the treatment should be a right hemicolectomy (40).

Right-sided Colonic Tumors.—Half of colonic carcinoid tumors arise in the cecum, and approximately 15% arise in the ascending colon (41). These tumors frequently are manifested by symptoms of pain, anorexia, and weight loss. Tumor size is greater than 2 cm in more than 90% of patients affected, and many patients have either nodal or distant metastases at diagnosis; even lesions with a diameter of less than 1 cm are associated with metastases in 22% of patients (6). Imaging features are indistinguishable from those of colonic adenocarcinoma at barium contrast studies (Fig 9a). At CT or MR imaging, there is typically circumferential thickening of the cecum (Fig 9b), which may be indistinguishable from that in cecal carcinoma, another tumor type that, like colonic carcinoid tumor, frequently metastasizes

Figure 10. Rectal carcinoid tumor. Axial T2-weighted high-resolution MR image demonstrates a tumor in the posterior rectal wall, with bilateral adjacent mesorectal nodal metastases (arrows). The rectal mass was a histologically proved carcinoid tumor.

to the liver or mesentery. Somatostatin receptor scintigraphy performed for preoperative staging often depicts metastatic disease.

Hindgut Carcinoid Tumors

Left-sided Colonic Tumors.—The left-sided colon is an uncommon tumor site, and only 10%–15% of all colorectal carcinoid tumors arise from the transverse, descending, or sigmoid colon (41). These tumors are associated with a poorer prognosis due to their typically advanced stage at presentation. Their imaging appearances are similar to those of colonic carcinoma.

Rectal Tumors.—Rectal carcinoid tumors are often small and asymptomatic and only detected coincidentally at colonoscopy (11,41). The size of a primary lesion correlates with the risk of metastasis, and small tumors (<1 cm) can be successfully treated with local resection (41). Larger tumors often have spread to regional nodes and the liver by the time the disease is diagnosed (Fig 10). Imaging modalities include cross-sectional techniques (CT and MR imaging), somatostatin receptor scintigraphy, and endoscopic US, the last of which can accurately depict the depth of invasion and perirectal nodal spread.

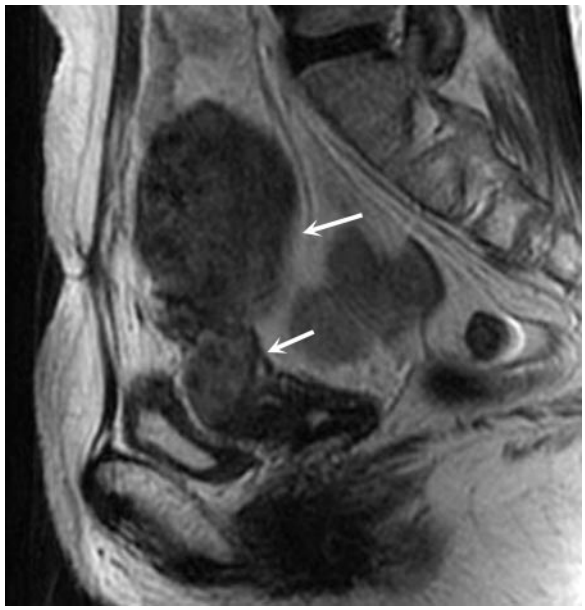

Figure 11. Cervical carcinoid tumor. Sagittal T2-weighted MR image shows a large mass that involves the uterus and cervix and extends into the endometrial cavity (arrows). Histologic analysis of a biopsy specimen revealed a poorly differentiated carcinoid tumor. A metastatic deposit in the sacrum (not shown) also was found at the time of diagnosis.

Ovarian Tumors.—Carcinoid tumors of the ovary are uncommon and usually arise from respiratory or gastrointestinal epithelial cells within a mature teratoma (42). Such tumors are relatively benign and rarely metastasize. Purely carcinoid ovarian tumors are exceedingly rare and tend to be more aggressive. Cross-sectional imaging typically demonstrates a large, solid, unilateral adnexal mass that is indistinguishable from other ovarian malignancies, and the diagnosis is achieved only after excision and histologic analysis (42).

Rare Primary Tumor Sites

Carcinoid tumors have been reported to arise from the gallbladder, kidney (7), heart, testis (9), and uterine cervix (43) (Fig 11). Imaging appearances are generally nonspecific and do not allow differentiation from more common pathologic entities. A diagnosis frequently can be made only after surgical excision.

Figure 12. Mesenteric metastases of carcinoid disease. **(a)** Coronal reformatted image from CT angiography of the mesenteric vessels shows a partly calcified mesenteric carcinoid deposit (arrow) that encases the distal superior mesenteric artery and ileal artery branch vessels. **(b)** Anterior planar image from whole-body scintigraphy performed with ^{111}In-octreotide in another patient demonstrates radiotracer uptake in a mesenteric carcinoid metastasis (arrow). **(c, d)** Axial SPECT images obtained with ^{111}In-octreotide in another patient demonstrate a solitary abnormal focus of radiotracer uptake in the midline (crosshairs). **(e, f)** Low-dose CT image **(e)** and SPECT/CT image **(f)** show a metastatic lymph node (crosshairs) just anterior to the body of the pancreas. The patient had undergone resection of an ileal carcinoid tumor 18 months previously, and levels of biochemical markers had since increased.

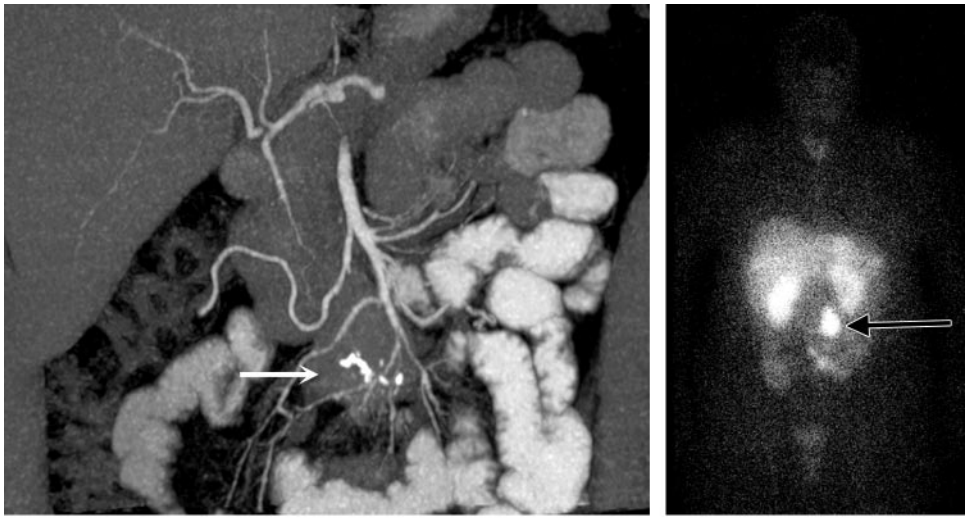

a. b.

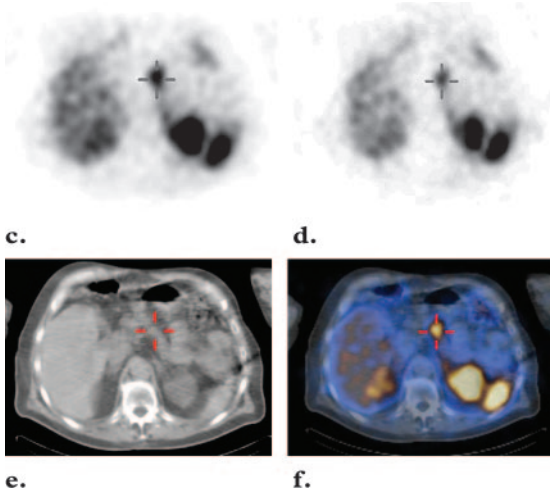

c. d. e. f.

Imaging of Metastatic Disease

The incidence of metastatic disease in patients with carcinoid tumors varies, depending on the primary site. Approximately 40%–80% of midgut carcinoid tumors spread to the small-bowel mesentery either by direct extension or via local lymph vessels (35). At CT, the usual appearance of mesenteric disease is an ill-defined enhancing soft-tissue mass that, in an estimated 70% of cases, contains calcification (Fig 12a) (35). Three-dimensional CT angiography can be useful to depict the full extent of mesenteric disease and the degree of involvement of vascular structures

Figure 13. Metastases to other intraabdominal organs. **(a)** Axial gadolinium-enhanced T1-weighted abdominal MR image shows a subtle focal lesion in the body of the pancreas (arrow). **(b)** Corresponding SPECT image from scintigraphy performed with ^{111}In-octreotide shows abnormal radiotracer uptake within the upper abdomen (arrow). **(c)** Fusion MR-SPECT image from a patient with a previous resection of primary ovarian carcinoid tumor and with increasing levels of biochemical markers shows the alignment of the two abnormalities (arrow), a finding indicative of an octreotide-avid metastatic deposit in the pancreatic body. **(d)** Axial contrast-enhanced CT image in a patient with an ileal carcinoid tumor demonstrates a left ovarian mass (arrow). After oophorectomy, the mass was histologically diagnosed as a carcinoid metastasis.

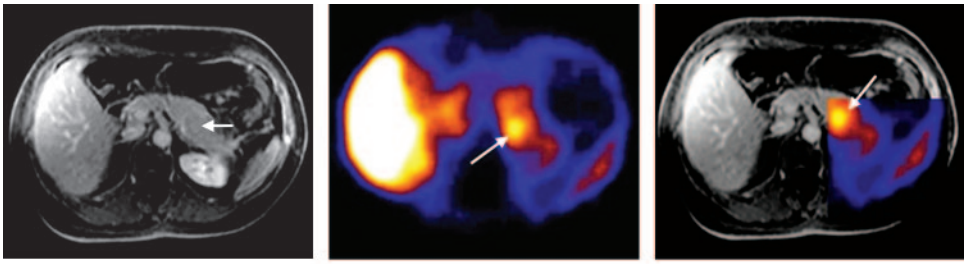

a. b. c.

d.

that may preclude surgical resection (Fig 12a) (34). Frequently, mesenteric deposits are strongly positive at octreotide scintigraphy (Fig 12b). The use of hybrid SPECT/CT systems (Fig 12c–12f) or the coregistration of data from functional imaging with data from cross-sectional imaging may lead to improved detection of smaller lesions (Fig 13a–13c).

Liver metastases are common. Characteristically, carcinoid metastases to the liver are hypervascular, and most can be detected easily on CT or MR images acquired immediately after contrast material administration (37) (Fig 14a, 14b). At MR imaging, hepatic metastases typically demonstrate low signal intensity on T1-weighted images (Fig 14c) and high signal intensity on T2-weighted images (Fig 14d) because of their complex cystic nature. Metastases usually show moderately intense enhancement during the hepatic arterial phase (37). Larger metastases may show heterogeneous enhancement due to central necrosis. Scintigraphy performed with octreotide or

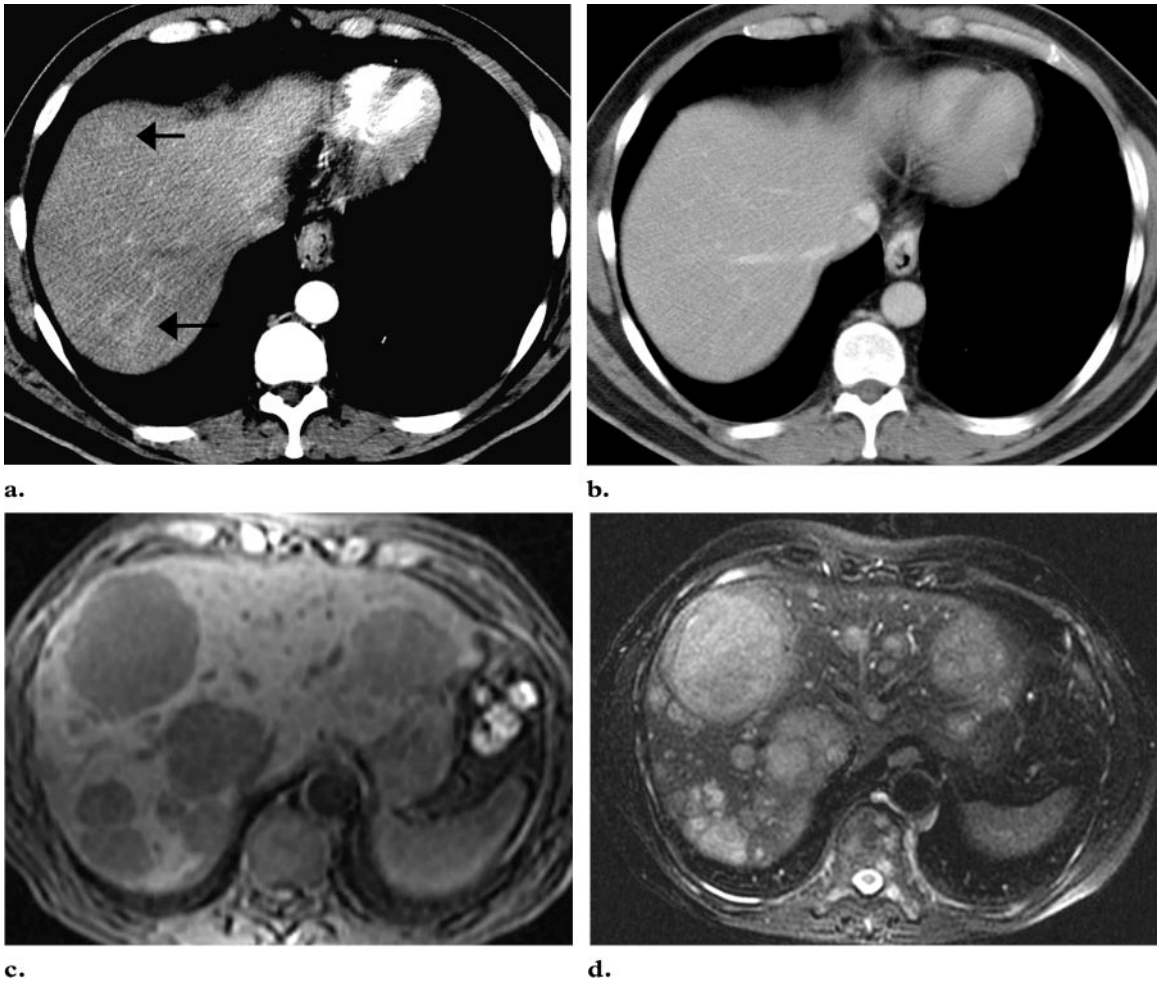

Figure 14. Hepatic metastases of carcinoid disease. **(a)** Contrast-enhanced arterial phase CT image shows avidly enhancing foci in the liver (arrows), features indicative of hepatic metastases in a patient with a gastric carcinoid tumor. **(b)** Contrast-enhanced portal phase CT image at the same level as **a** shows no foci of enhancement. **(c, d)** Axial T1-weighted MR image **(c)** and T2-weighted MR image **(d)** show regions of low T1-weighted signal intensity and high T2-weighted signal intensity, respectively, findings typical of carcinoid liver metastases.

iobenguane I 123 frequently demonstrates radiotracer uptake within liver metastases, unless the lesions are predominantly cystic (Fig 15b).

Carcinoid tumors occasionally metastasize to other intraabdominal organs. Pancreatic metastases appear as focal pancreatic masses that may show increased metabolic activity at functional imaging (Fig 13a–13c). Up to 2% of gastrointestinal carcinoid tumors may metastasize to the ovaries and produce adnexal masses (44) (Fig 13d). Pulmonary, pleural, and mediastinal metastatic disease is less common, except in patients with thymic carcinoid tumors, in whom the malignancy often has spread to these sites by the time of presentation or in whom a primary tumor may recur with pleural and mediastinal deposits (Fig 1b).

Metastases to bone are relatively uncommon in carcinoid disease (7%–15% of all metastases), arise more commonly from foregut primary tumors, and frequently are manifested by bone pain

a. b.

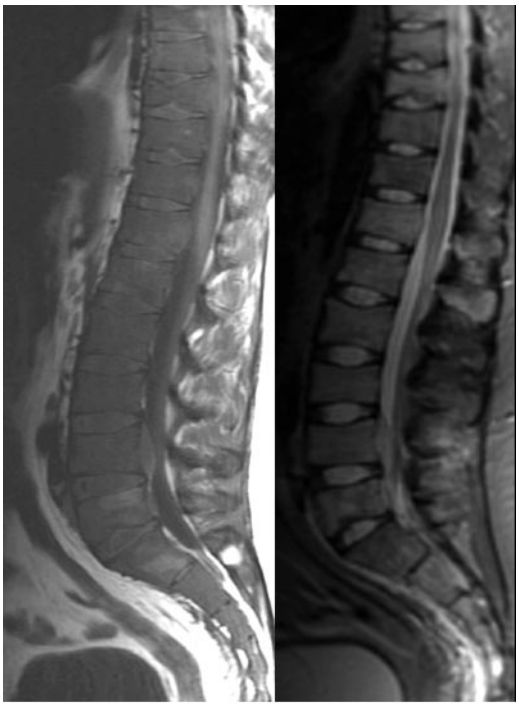

c.

Figure 15. Metastases to bone. **(a)** Axial CT image obtained with bone window settings in a patient with metastatic bronchial carcinoid tumor demonstrates a sclerotic bone metastasis in the right iliac bone (arrow). **(b)** Planar images from bone scintigraphy (left), iobenguane I 123 scintigraphy (middle), and ^{111}In-octreotide scintigraphy (right) obtained in the same patient over a 3-month period demonstrate multiple metastases to bone. The iobenguane scintigram is floridly abnormal, showing multiple foci of radiotracer uptake in the liver and throughout the marrow-containing bones. These features are less conspicuous on the other two images. **(c)** Sagittal MR images, obtained in another patient with a T1-weighted sequence (left) and a short inversion time inversion recovery sequence (right), depict multiple intravertebral foci of high T1-weighted and low T2-weighted signal intensity, respectively. These findings are indicative of metastases from an ileal carcinoid tumor.

(45). Radiographic signs may be subtle and easily missed. CT images may demonstrate sclerotic bone lesions (Fig 15a). MR imaging is the most sensitive method of detecting metastases in bone marrow, with a sensitivity of nearly 100% (45). The MR imaging appearance of lesions may be identical to that of bone metastases from other primary tumors, and if marrow deposits are sclerotic, they may show low signal intensity on T2-weighted images (Fig 15c). Bone scintigraphy is a sensitive and reliable method for the detection of carcinoid metastases to bone, with a sensitivity of 90% (45). Scintigraphy performed with iobenguane, octreotide, or both also may be useful (Fig 15b); however, despite the high sensitivity of these methods for the detection of metastatic disease in other anatomic regions, the use of radiotracers may lead to underestimation of, or failure to detect, tumor deposits in bone in 50%–80% of cases (46).

Teaching Point

With recent advances in functional and anatomic imaging and the increased survival time made possible by new treatment modalities, more unusual sites of metastatic disease occasionally are seen. Such sites include the soft tissues (17) (Fig 16a), breasts, heart, skull (Fig 16b), and orbits (19) (Fig 16c).

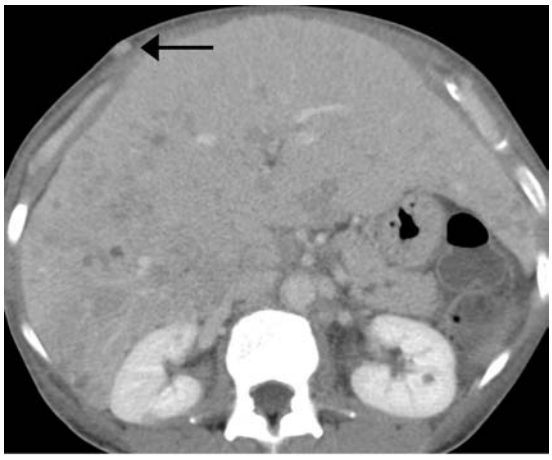

a.

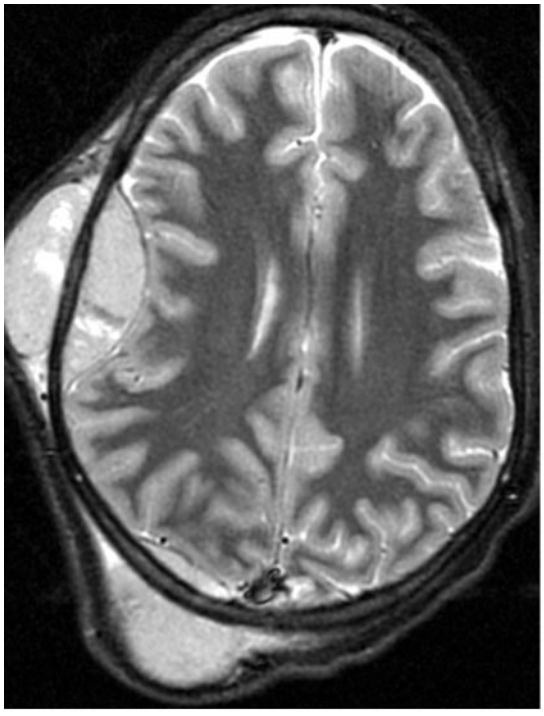

b.

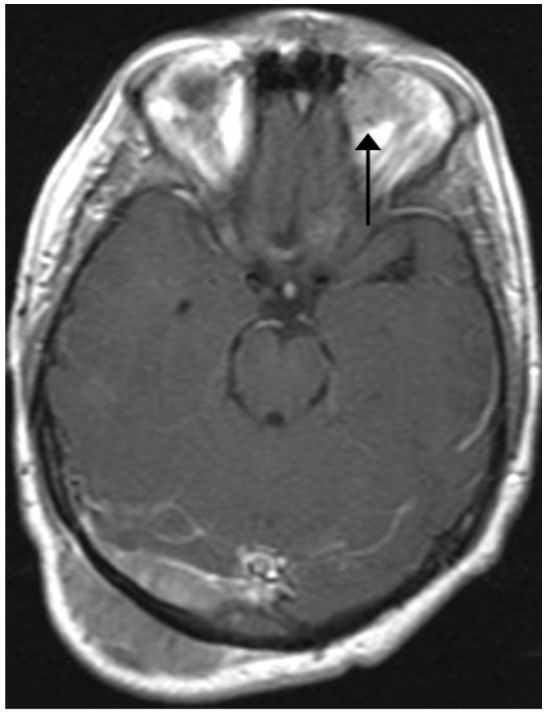

c.

Figure 16. Unusual sites of metastatic disease. **(a)** Contrast-enhanced CT image in a patient with advanced metastatic carcinoid disease demonstrates an enhancing nodule in the right anterior abdominal soft tissues, a finding consistent with a metastatic deposit (arrow). Marked hepatomegaly due to multiple liver metastases and ascites also is visible. **(b)** Axial T2-weighted MR image shows right parietal and occipital soft-tissue masses that traverse the calvaria in a patient with an end-stage thymic carcinoid tumor. The masses were histologically proved carcinoid metastases. **(c)** Gadolinium-enhanced T1-weighted MR image depicts an intraconal, retro-orbital metastasis (arrow) within the superomedial aspect of the left orbit.

Imaging of Carcinoid Heart Disease

Carcinoid heart disease, which occurs as part of the carcinoid syndrome, is characterized by plaquelike intracardiac deposits of fibrous tissue in the right heart valves and endocardium, with resultant valvular dysfunction and, in severe cases, right heart failure (47). Echocardiography is most commonly used to identify carcinoid heart disease. Right atrial and right ventricular enlargement is present in up to 90% of cases, and ventricular septal wall motion abnormalities are seen in almost 50% of cases (47). The tricuspid valve leaflets and subvalvar structures often are thickened, shortened, and retracted; these conditions lead to incomplete valve closure and, usually, moderate or severe tricuspid regurgitation (Fig 17). Right chamber enlargement may be demonstrable at cross-sectional imaging. MR imaging has an advantage over CT because tricuspid valve motion and valvular dysfunction can be precisely assessed and quantified by using cine MR imaging in combination with velocity encoding (48).

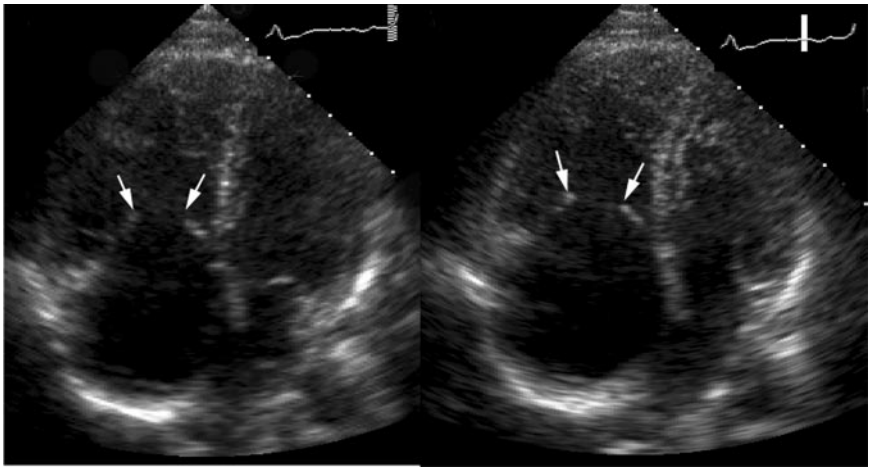

Figure 17. Carcinoid heart disease. Left: Cardiac US image in a patient with carcinoid syndrome due to a metastatic ileal carcinoid tumor shows the tricuspid valve (arrows) during diastole, and the electrocardiographic tracing shows that image acquisition occurred on the R wave, immediately before right ventricular contraction. Right: Cardiac US image shows the tricuspid valve (arrows) during systole, and the electrocardiographic tracing shows that image acquisition occurred during systole. The tricuspid valve appears fixed; the right ventricle has contracted, but the immobile valve remains wide open. The consequence is severe tricuspid regurgitation. (Courtesy of Robin Choudhury, MD, Department of Cardiovascular Medicine, University of Oxford.)

Combined Cross-sectional and Functional Imaging

A combination of cross-sectional and functional imaging techniques is vital for initial staging, disease monitoring, assessment of therapeutic response, and detection of new manifestations of carcinoid tumors. The contribution of each imaging technique varies according to the primary tumor site. High-resolution contrast-enhanced CT and MR imaging are excellent for detection of larger primary tumors and metastatic disease (Figs 13, 14). Endoscopic US may demonstrate small gastric, duodenal, or rectal carcinoid tumors that otherwise might not be detected (Fig 5).

Teaching Point

Functional imaging complements cross-sectional imaging, and because most carcinoid tumors express somatostatin receptors, somatostatin receptor scintigraphy is widely used as the primary imaging method for diagnosis, staging, and monitoring of carcinoid tumors (49,50). Somatostatin receptor scintigraphy performed with ^{111}In-octreotide is a sensitive method of localizing radiologically occult carcinoid tumors, with a reported sensitivity of 80%–100% (51) (Figs 2d, 12b, 12c–12f, 13a–13c, 15b). This whole-body imaging technique may provide valuable information about unsuspected metastatic disease. Octreotide scintigraphy may depict tumor deposits as small as 6 mm in diameter when single photon emission CT (SPECT) data also are obtained (52). Somatostatin receptor scintigraphy is important also for assessing patients' suitability for radiolabeled somatostatin analog therapy and for monitoring the response to that therapy.

Scintigraphy with iobenguane I 123 has been used for many years to visualize carcinoid tumors but has a lower sensitivity (36%–85%) than does somatostatin receptor scintigraphy (Fig 15b) (53). Iobenguane scintigraphy is particularly useful when other methods have failed to depict carcinoid tumors or when treatment with iobenguane I 131 is being considered. Carcinoid tumors and metastases may show similar or variable affinity for different radiotracers. As a result, no one functional imaging test is perfect, and a combination of different imaging modalities helps to provide a comprehensive map of disease (54).

Teaching Point

Computer-assisted image fusion of cross-sectional (anatomic) and scintigraphic (functional) image data has been shown to increase the accuracy of tumor and metastatic disease localization (Fig 13a–13c) (55). Hybrid CT/gamma camera systems recently have been introduced, and this new technology has been shown to be highly accurate for localization of tumors and metastases (Fig 12c–12f) (56). At present, the quality of the CT component of hybrid systems is not sufficient to allow hybrid imaging to replace dedicated CT or MR imaging, and the side-by-side comparison of functional and anatomic images remains a key component in the evaluation of neuroendocrine tumors (57).

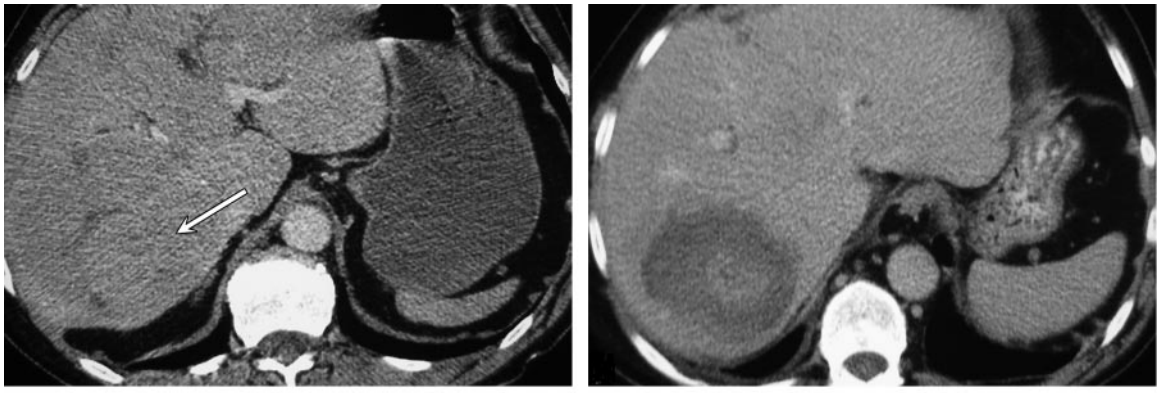

a. b.

Figure 18. Ablation of hepatic metastases. **(a)** Axial contrast-enhanced CT image, obtained before ablation, shows a large and poorly defined carcinoid metastasis in the right lobe of the liver (arrow). **(b)** Postprocedural CT image shows an extensive low-attenuation region within the tumor, a feature that signifies technically successful ablation. The patient experienced a marked improvement in symptoms after ablation therapy.

Despite the increasing role of PET in oncologic imaging, this modality does not currently play a major role in the imaging of carcinoid tumors. Most carcinoid tumors are well differentiated and slow growing and have a low metabolic rate. As a result, the radiotracer most commonly used in oncologic imaging, FDG, is not localized within most carcinoid tumors (26). Increased FDG uptake may be seen in more aggressive, poorly differentiated tumors (Fig 6b), which are less likely to have somatostatin receptors and to be depicted at somatostatin receptor scintigraphy (53). Other PET radiotracers, such as carbon 11–5-hydroxytryptophan (58), copper 64–tetraazocyclotetradecane octreotide (59), fluorodopa F 18 (60), and gallium 68–tetraazocyclododecane tetraacetic acid octreotide (61), show promise for future use in the evaluation of neuroendocrine tumors. However, these radiotracers are available in only a few highly specialized centers.

Current Treatment of Carcinoid Disease

An increasing number of therapeutic options are available to patients with carcinoid disease. Although surgery remains the only curative treatment, significant relief of symptoms and improvements in the quality of life and long-term survival of patients with metastatic disease can be achieved by combining various treatment modalities. Medical treatment options include cytotoxic agents, interferon-α, and somatostatin analogs. Somatostatin analogs are well tolerated, help reduce clinical symptoms, and may help stabilize disease in most patients (62). Chemotherapy may be most useful in patients with aggressive tumors, whereas interferon-α is more beneficial in classic low-grade midgut carcinoid tumors when used in combination with a somatostatin analog (12). Liver ablative procedures such as embolization, chemoembolization (embolization combined with intraarterial chemotherapy), and radiofrequency ablation reduce the tumor burden from metastatic disease in the liver, provide a marked improvement in symptoms, and increase life expectancy (63). Promising results have been shown with the use of new tumor-targeted radiolabeled iobenguane and somatostatin analog therapies (64). The complexity of carcinoid disease and the spectrum of therapeutic options reinforce the need for multidisciplinary collaboration among clinicians, radiologists, surgeons, and oncologists to optimize management.

Disease Monitoring and Assessment of Treatment Response

Increasingly, imaging plays a pivotal role in disease monitoring and assessment of tumor response to various treatments.

After undergoing treatment, patients typically are examined annually with cross-sectional imaging (most commonly MR imaging) to document the number and size of lesions and detect disease response, stability, or progression. If there is an increase in the levels of biochemical tumor markers or a generalized deterioration in the patient's status, a more immediate imaging evaluation may be required. In addition, information from serial

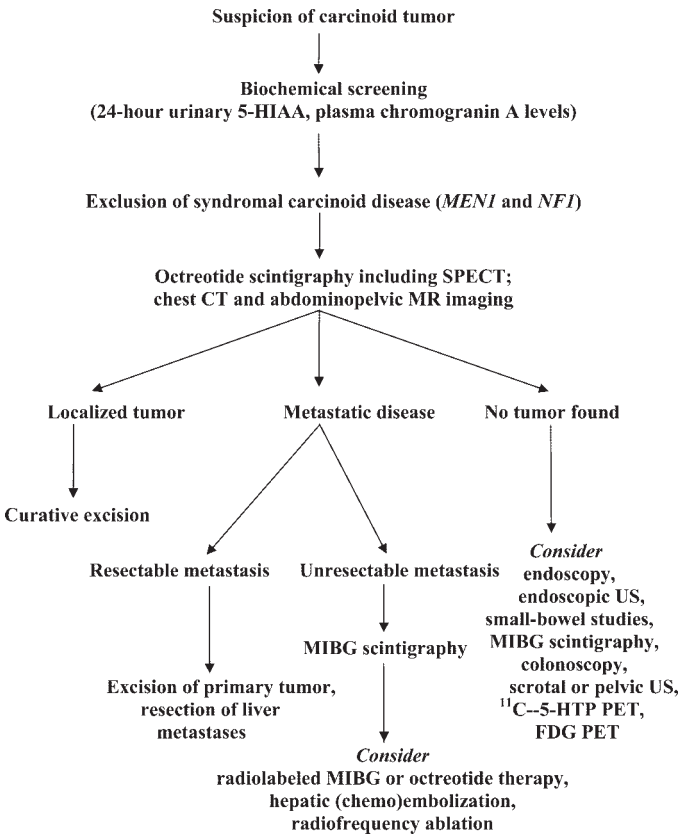

Figure 19. Flow chart shows the suggested imaging protocol for evaluating patients in whom the presence of a carcinoid tumor is suspected. *^{11}C–5-HTP* = carbon 11–5-hydroxytryptophan, *5-HIAA* = 5-hydroxyindolacetic acid.

scintigraphic examinations with iobenguane I 123 or iobenguane I 131 and with ^{111}In-octreotide may be used to assess the response to radionuclide treatment, especially in cases in which lesions were not depicted on cross-sectional images. In our experience, a marked improvement in symptoms often is observed after interventional or radionuclide therapy for metastatic carcinoid tumors, but rarely is any significant structural change seen on cross-sectional images. In many cases, a period of stabilization is followed by a slow progression of disease.

The use of certain treatment modalities requires specific imaging evaluations both before and after treatment. These modalities are described in the next two sections.

Radionuclide Therapy

A prerequisite for radionuclide therapy is a positive finding at iobenguane or octreotide scintigraphy. After systemic administration of iobenguane I 131 or yttrium 90–octreotide, a whole-body scintigram is obtained to demonstrate any uptake of the radiotracer and document any disease sites. This scintigram is used as a baseline for future comparisons.

Ablative Treatments for Hepatic Metastases

Both embolization and radiofrequency ablation result in tumor necrosis and in a reduction of tumor bulk and are accompanied by a marked improvement of symptoms in most patients. A comparison of preoperative (Fig 18a) and postoperative (Fig 18b) cross-sectional images is very useful to assess therapeutic success and to exclude complications.

Suggested Imaging Algorithms in Carcinoid Disease

Radiologic and radionuclide imaging play a vital role in the management of patients with carcinoid tumors and can be tailored to each case. A number of useful guidelines for the diagnosis and treatment of a wide variety of neuroendocrine tumors are available (65–68). There are two key aspects: *(a)* primary diagnosis and staging in patients in whom carcinoid disease is suspected (localization of the primary site and detection of any metastatic disease is crucial, as this determines the feasibility of resection, the only curative treatment) (Fig 19);

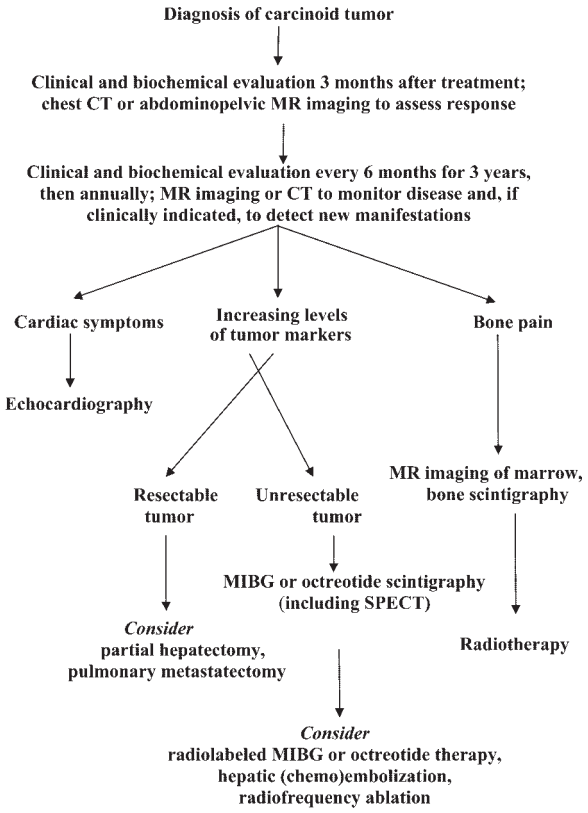

Figure 20. Flow chart shows the recommended procedures for disease monitoring, assessment of treatment response, and detection of new or recurrent lesions after an initial diagnosis of carcinoid tumor.

and *(b)* monitoring of known carcinoid disease, assessment of response to treatment, and detection of new manifestations (Fig 20). The imaging protocols used in our department are adapted from the clinical practice guidelines published by the National Comprehensive Cancer Network (69).

Conclusions

Imaging plays a central role in the initial evaluation and follow-up of patients with carcinoid tumors. An understanding of the spectrum of disease and the contribution of different imaging techniques is essential for accurate detection, staging, and surveillance in this diverse patient group.

References

1. Taal BG, Visser O. Epidemiology of neuroendocrine tumours. Neuroendocrinology 2004;80:3–7.
2. Eriksson B, Oberg K. Carcinoid syndrome. In: DeGroot L, Jameson LJ, eds. Endocrinology. 5th ed. Philadelphia, Pa: Saunders, 2005; 3571–3584.
3. Zuetenhorst JM, Taal BG. Metastatic carcinoid tumors: a clinical review. Oncologist 2005;10: 123–131.
4. Williams ED, Sandler M. The classification of carcinoid tumours. Lancet 1963;1:238–239.
5. Solcin E, Klippel G, Sobin L, eds. Histological typing of endocrine tumors. New York, NY: Springer, 2000; 38–74.
6. Kulke MH, Mayer RJ. Carcinoid tumors. N Engl J Med 1999;340(11):858–868.
7. Mufarrij P, Varkarakis IM, Studeman KD, Jarrett TW. Primary renal carcinoid tumor with liver metastases detected with somatostatin receptor imaging. Urology 2005;65:1002.
8. Riddell DA, LeBoldus GM, Joseph MG, Hearn SA. Carcinoid tumour of the middle ear: case report and review of the literature. J Otolaryngol 1994;23:276–280.
9. Frank RG, Gerard PS, Anselmo MT, Bennett L, Perminger BI, Wise GJ. Primary carcinoid tumor of the testis. Urol Radiol 1991;12:203–205.
10. Caplin ME, Buscombe JR, Hilson AJ, Jones AL, Watkinson AF, Burroughs AK. Carcinoid tumour. Lancet 1998;352:799–805.
11. Kaltsas GA, Besser GM, Grossman AB. The diagnosis and medical managment of advanced neuroendocrine tumors. Endocr Rev 2004;25(3): 458–511.
12. Oberg K. Management of neuroendocrine tumours. Ann Oncol 2004;15(suppl 4):293–298.
13. Modlin IM, Lye KD, Kidd M. A 5-decade analysis of 13,715 carcinoid tumors. Cancer 2003;97: 934–959.
14. Schnirer II, Yao JC, Ajani JA. Carcinoid: a comprehensive review. Acta Oncol 2003;42(7):672–692.
15. Moller JE, Pellikka PA, Bernheim AM, Schaff HV, Rubin J, Connolly HM. Prognosis of carcinoid heart disease: analysis of 200 cases over two decades. Circulation 2005;112:3320–3327.
16. Westberg G, Wangberg B, Ahlman H, et al. Prediction of prognosis by echocardiography in patients with midgut carcinoid syndrome. Br J Surg 2001;88:865–872.
17. Quan GM, Pitman A, Slavin J, Zalcberg J, Choong PF. Soft tissue metastasis of carcinoid tumour: a rare manifestation. ANZ J Surg 2004; 74:164–166.
18. Kaltsas GA, Putignano P, Mukherjee JJ, et al. Carcinoid tumours presenting as breast cancer: the utility of radionuclide imaging with ^{123}I-MIBG and ^{111}In-DTPA pentetreotide. Clin Endocrinol (Oxf) 1998;49:685–689.
19. Isidori AM, Kaltsas G, Frajese V, et al. Ocular metastases secondary to carcinoid tumors: the utility of imaging with ^{123}I-MIBG and ^{111}In-DTPA pentetreotide. J Clin Endocrinol Metab 2002;87: 1627–1633.
20. Rosado de Christenson ML, Abbott GF, Kirejczyk WM, Galvin JR, Travis WD. Thoracic carcinoids: radiologic-pathologic correlation. RadioGraphics 1999;19:707–736.
21. Moran CA, Suster S. Neuroendocrine carcinomas of the thymus: a clinicopathologic analysis of 80 cases. Am J Clin Pathol 2000;114:100–110.
22. Birnberg FA, Webb WR, Selch MT, Gamsu G, Goodman PC. Thymic carcinoid tumors with hyperparathyroidism. AJR Am J Roentgenol 1982; 139:1001–1004.
23. Hage R, Brutel de la Riviere A, Seldenrijk CA, van den Bosch JM. Update in pulmonary carcinoid tumors: a review article. Ann Surg Oncol 2003; 10(6):697–704.
24. Chong S, Lee KS, Chung MJ, Han J, Kwon OJ, Kim TS. Neuroendocrine tumors of the lung:

clinical, pathologic, and imaging findings. RadioGraphics 2006;26:41–58.
25. Jeung MY, Gasser B, Gangi A, et al. Bronchial carcinoid tumors of the thorax: spectrum of radiologic findings. RadioGraphics 2002;22:351–365.
26. Adams S, Baum R, Rink T, et al. Limited value of fluorine-18-fluorodeoxyglucose positron emission tomography for the imaging of neuroendocrine tumors. Eur J Nucl Med 1998;25:79–83.
27. Binstock AJ, Johnson CD, Stephens DH, Lloyd RV, Fletcher JG. Carcinoid tumors of the stomach: a clinical and radiographic study. AJR Am J Roentgenol 2001;176:947–951.
28. Delle Fave G, Capurso G, Annibale B, Panzuto F. Gastric neuroendocrine tumors. Neuroendocrinology 2004;80:16–19.
29. Levy AD, Taylor LD, Abbott RM, Sobin LH. Duodenal carcinoids: imaging features with clinical-pathologic comparison. Radiology 2005;237:967–972.
30. Zimmer T, Scherübl H, Faiss S, Stölzel U, Riecken EO, Wiedenmann B. Endoscopic ultrasonography of neuroendocrine tumours. Digestion 2000;62:45–50.
31. Iwao M, Nakamuta M, Enjoji M, et al. Primary hepatic carcinoid tumor: case report and review of 53 cases. Med Sci Monit 2001;7(4):746–750.
32. Migliori M, Tomassetti P, Lalli S, et al. Carcinoid of the pancreas. Pancreatology 2002;2:163–166.
33. Horton KM, Kamel I, Hofmann L, Fishman EK. Carcinoid tumors of the small bowel: a multitechnique imaging approach. AJR Am J Roentgenol 2004;182:559–567.
34. Gore RM, Berlin JW, Mehta UK, Newmark GM, Yaghmai V. GI carcinoid tumours: appearance of the primary and detecting metastases. Best Pract Res Clin Endocrinol Metab 2005;19(2):245–263.
35. Pantongrag-Brown L, Buetow PC, Carr NJ, Lichtenstein JE, Buck JL. Calcification and fibrosis in mesenteric carcinoid tumor: CT findings and pathologic correlation. AJR Am J Roentgenol 1995;164:387–391.
36. Sheth S, Horton KM, Garland MR, Fishman EK. Mesenteric neoplasms: CT appearances of primary and secondary tumors and differential diagnosis. RadioGraphics 2003;23:457–473.
37. Bader TR, Semelka RC, Chiu VC, Armao DM, Woosley JT. MRI of carcinoid tumors: spectrum of appearances in the gastrointestinal tract and liver. J Magn Reson Imaging 2001;14:261–269.
38. Kvols L. Carcinoids of the appendix. Neuroendocrinology 2004;80:33–34.
39. Pickhardt PJ, Levy AD, Rohrmann CA Jr, Kende AI. Primary neoplasms of the appendix: radiologic spectrum of disease with pathologic correlation. RadioGraphics 2003;23:645–662.
40. Moertel CG, Weiland LH, Nagomey DM, Dockerty MB. Carcinoid tumor of the appendix: treatment and prognosis. N Engl J Med 1987;317:1699–1701.
41. Vogelsang H, Siewert JR. Endocrine tumours of the hindgut. Best Pract Res Clin Gastroenterol 2005;19(5):739–751.
42. Outwater EK, Siegelman ES, Hunt JL. Ovarian teratomas: tumor types and imaging characteristics. RadioGraphics 2001;21:475–490.
43. Okamoto Y, Tanaka YO, Nishida M, Tsunoda H, Yoshikawa H, Itai Y. MR imaging of the uterine cervix: imaging-pathologic correlation. RadioGraphics 2003;23:425–445.
44. Robboy SJ, Scully RE, Norris HJ. Carcinoid metastatic to the ovary: a clinicopathologic analysis of 35 cases. Cancer 1974;33(3):798–811.
45. Meijer WG, van der Veer E, Jager PL, et al. Bone metastases in carcinoid tumors: clinical features, imaging characteristics, and markers of bone metabolism. J Nucl Med 2003;44(2):184–191.
46. Zuetenhorst JM, Hoefnageli CA, Boot H, Valdés Olmos RA, Taal BG. Evaluation of 111In-pentetreotide, 131I-MIBG and bone scintigraphy in the detection and clinical management of bone metastases in carcinoid disease. Nucl Med Commun 2002;23:735–741.
47. Fox DJ, Khattar RS. Carcinoid heart disease: presentation, diagnosis and management. Heart 2004;90:1224–1228.
48. Mollet NR, Dymarkowski S, Bogaert J. MRI and CT revealing carcinoid heart disease. Eur Radiol 2003;13(suppl 6):L14–L18.
49. Reubi JC. Somatostatin and other peptide receptors as tools for tumor diagnosis and treatment. Neuroendocrinology 2004;80:51–56.
50. Low MJ. The somatostatin neuroendocrine system: physiology and clinical relevance in gastrointestinal and pancreatic disorders. Best Pract Res Clin Endocrinol Metab 2004;18(4):607–622.
51. Kaltsas G, Rockall A, Papadogias D, Resnek R, Grossman AB. Recent advances in radiological and radionuclide imaging and therapy of neuroendocrine tumours. Eur J Endocrinol 2004;151:15–27.
52. Oberg K, Eriksson B. Nuclear medicine in the detection, staging and treatment of gastrointestinal carcinoid tumours. Best Pract Res Clin Endocrinol Metab 2005;19(2):265–276.
53. Ezziddin S, Logvinski T, Yong-Hing C, et al. Factors predicting tracer uptake in somatostatin receptor and MIBG scintigraphy of metastatic gastroenteropancreatic neuroendocrine tumors. J Nucl Med 2006;47:223–233.
54. Kaltsas G, Korbonits M, Heintz E, et al. Comparison of somatostatin analog and MIBG radionuclides in the diagnosis and localization of advanced neuroendocrine tumors. J Clin Endocrinol Metab 2001;86:895–902.
55. Amthauer H, Denecke T, Rohlfing T, et al. Value of image fusion using single photon emission computed tomography with integrated low dose computed tomography in comparison with a retrospective voxel-based method in neuroendocrine tumours. Eur Radiol 2005;15:1456–1462.
56. Krausz Y, Keidar Z, Kogan I, et al. SPECT/CT hybrid imaging with ^{111}In-pentetreotide in assessment of neuroendocrine tumours. Clin Endocrinol (Oxf) 2003;59:565–573.
57. Pfannenberg AC, Eschmann SM, Horger M, et al. Benefit of anatomical-functional image fusion in the diagnostic work-up of neuroendocrine neoplasms. Eur J Nucl Med Mol Imaging 2003;30:835–843.
58. Orlefors H, Sundin A, Garske U, et al. Whole-body ^{11}C-5-hydroxytryptophan positron emission tomography as a universal imaging technique for neuroendocrine tumors: comparison with somatostatin receptor scintigraphy and computed tomography. J Clin Endocrinol Metab 2005;90:3392–3400.

59. Anderson CJ, Dehdashti F, Cutler PD, et al. ^{64}Cu-TETA-octreotide as a PET imaging agent for patients with neuroendocrine tumors. J Nucl Med 2001;42:213–221.
60. Hoegerle S, Altehoefer C, Ghanem N, et al. Whole-body ^{18}F dopa PET for detection of gastrointestinal carcinoid tumors. Radiology 2001;220:373–380.
61. Bohuslavizki KH. Somatostatin receptor imaging: current status and future perspectives. J Nucl Med 2001;42:1057–1058.
62. Welin SV, Janson ET, Sundin A, et al. High-dose treatment with a long-acting somatostatin analogue in patients with advanced midgut carcinoid tumours. Eur J Endocrinol 2004;151:107–112.
63. Ruszniewski P, O'Toole D. Ablative therapies for liver metastases of gastroenteropancreatic endocrine tumors. Neuroendocrinology 2004;80(suppl 1):74–78.
64. Pasieka JL, McEwan AJ, Rorstad O. The palliative role of 131I-MIBG and 111In-octreotide therapy in patients with metastatic progressive neuroendocrine neoplasms. Surgery 2004;136:1218–1226.
65. Oberg K, Astrup L, Eriksson B, et al. Guidelines for the management of gastroenteropancreatic neuroendocrine tumours (including bronchopulmonary and thymic neoplasms). Part I. General overview. Acta Oncol 2004;43(7):617–625.
66. Oberg K, Astrup L, Eriksson B, et al. Guidelines for the management of gastroenteropancreatic neuroendocrine tumours (including bronchopulmonary and thymic neoplasms). Part II. Specific NE tumour types. Acta Oncol 2004;43(7):626–636.
67. Plockinger U, Rindi G, Arnold R, et al. Guidelines for the diagnosis and treatment of neuroendocrine gastrointestinal tumours: a consensus statement on behalf of the European Neuroendocrine Tumour Society (ENETS). Neuroendocrinology 2004;80:394–424.
68. Ricke J, Klose KJ, Mignon M, Oberg K, Wiedenmann B. Standardisation of imaging in neuroendocrine tumours: results of a European delphi process. Eur J Radiol 2001;37:8–17.
69. Neuroendocrine tumors. In: Clinical practice guidelines in oncology. Version 2.2006. National Comprehensive Cancer Network Web site. http://www.nccn.org/professionals/physician_gls/PDF/neuroendocrine.pdf. Accessed December 8, 2006.

Anatomic and Functional Imaging of Metastatic Carcinoid Tumors

Andrew F. Scarsbrook, MD et al

RadioGraphics 2007; 27:455–476 • **Published online** 10.1148/rg.272065058 • **Content Codes:** GI NM OI

Page 456
Neuroendocrine tumors may arise in a wide range of organs, but they most commonly arise in the submucosa of the bronchopulmonary and gastrointestinal tracts. Carcinoid tumors are a subgroup of midgut neuroendocrine tumors that secrete serotonin (5-hydroxytryptamine). Although the terms neuroendocrine tumor and carcinoid tumor are often used interchangeably, in this review we generally have used the term carcinoid tumor to describe that specific entity. Approximately 20% of patients with carcinoid tumors have metastatic disease at presentation, and in half of those patients the primary tumor is not located at initial imaging.

Page 457
Carcinoid tumors are relatively slow growing, and, even in the presence of metastatic disease, patients can survive for several years with current treatment strategies. The overall 5-year survival rate (regardless of tumor site or stage) approaches 70%–80%.

Page 469
With recent advances in functional and anatomic imaging and the increased survival time made possible by new treatment modalities, more unusual sites of metastatic disease occasionally are seen. Such sites include the soft tissues (Fig 16a), breasts, heart, skull (Fig 16b), and orbits (Fig 16c).

Page 471
High-resolution contrast-enhanced CT and MR imaging are excellent for detection of larger primary tumors and metastatic disease (Figs 13, 14). Endoscopic US may demonstrate small gastric, duodenal, or rectal carcinoid tumors that otherwise might not be detected (Fig 5).

Page 471
Carcinoid tumors and metastases may show similar or variable affinity for different radiotracers. As a result, no one functional imaging test is perfect, and a combination of different imaging modalities helps to provide a comprehensive map of disease.